

AUTOMATIC EXTRACTION OF TREES FROM AERIAL IMAGERY

W. Mayr¹, H. Mayer², U. Bacher², H. Ebner¹

¹Chair for Photogrammetry and Remote Sensing
Technische Universität München
D-80290 München, Germany

Ph.: +49-89-289-22671, Fax: +49-89-2809573

e-mail: willi@photo.verm.tu-muenchen.de, ebn@photo.verm.tu-muenchen.de

²Institute for Photogrammetry and Cartography
University of the Federal Armed Forces Munich
D-85577 Neubiberg, Germany

Ph.: +49-89-6004-3455, Fax: +49-89-6004-4090

e-mail: helmut.mayer@unibw-muenchen.de, uwe.bacher@unibw-muenchen.de

Semantische Modellierung; *SMATI 99*

KEY WORDS: Vegetation Extraction, High Resolution Aerial Imagery, Modeling

ABSTRACT

We present two approaches for the automatic extraction of trees from high resolution aerial imagery. In the first approach we aim at isolated trees in rural areas. This approach is based on automatically generated digital surface models (DSM). It models trees as generalized ellipsoids of revolution which are fitted to the DSM. The parameters of the generated generalized ellipsoids of revolution are then used to determine if they represent deciduous or coniferous trees. In the second approach we try to extract leafless deciduous trees from images of urban areas captured in spring. We make use of the dark shadows of trees as well as of the fact that the vertical trunks are imaged as nadir pointing straight lines. The Hough transform is employed to generate hypotheses for the trunks. Branches are tracked by means of hysteresis thresholding. With this approach it is possible to determine the trunk base, height, width, and outline of the tree. First results show the feasibility of both approaches.

1 INTRODUCTION

The extraction of trees from high resolution aerial imagery is a great challenge due to their complex structure and their interaction with other trees as well as other objects, such as buildings and roads. As there is a need for data about trees for forest management, cadastre, and three-dimensional (3D) city models, it is worth to take up this challenge.

Only few work deals with the automatic extraction of individual trees from aerial imagery. In [Larsen, 1998] which is the successor of [Pollock, 1996], trees are modeled by a generalized ellipsoid of revolution and a distribution function for the density of the branches and leaves. This model is used to generate templates of the trees, taking the geometry of the sensor, the time of data capture, the illumination, as well as the reflectance of the tree and the ground into account. The templates are varied concerning sizes and shapes of the trees and are matched with the imagery, in this case from a line scanner with 30 cm ground resolution. The disadvantage of the approach is that it works well only for imagery containing mostly trees, i.e., forest. Moreover, many templates are nec-

essary if the variability of trees is big. The approach proposed in [Brandtberg, 1996] is based on color-infrared imagery with a ground pixel size of about 3 cm. The approach uses information about the structure to classify the tree. Second order derivatives result into lines which are used to describe the branching structure. From the distribution of the orientations of the lines, a parallel structure can be distinguished from a radial structure. Herewith it is possible to classify three tree types: pine, spruce, and birch. This approach works, however, only in case the regions for the tree crowns are given.

Compared to these two approaches, we go into two different directions: We try to extract isolated single trees in rural areas and individual trees in urban areas. The reason for the former is that trees are important for landscape planning and because they can be context for road extraction [Baumgartner, 1998]. Opposed to this, trees in urban areas are of specific interest for cadastre and 3D city models. Our data source is in both cases high resolution aerial imagery with given orientation parameters. For the rural areas, the images were taken in summer as the leaves result into a prominent 3D structure then. For the urban

areas, the images were taken in spring because this imagery can be used for a wide variety of applications. In this part of the year deciduous trees, which form the majority of trees in urban areas, are leafless. As conifers are rarely found in public space and are therefore not so important for urban planning, our work in urban areas is limited to (leafless) deciduous trees.

The paper is split into two main parts. In Section 2 focusing on the extraction of isolated trees in rural areas from automatically generated digital surface models (DSM), trees are modeled as generalized ellipsoids of revolution with a radiometric representation by a density function for the tree crown (cf. Subsection 2.1). The actual extraction is based on a strategy proposed in Subsection 2.2. After presenting results of an investigation in Subsection 2.3, the approach is assessed in Subsection 2.4. The second part in Section 3 starts with setting up a model for leafless deciduous trees in urban areas which are represented both, directly and by their shadows in the images (cf. Subsection 3.1). It gives way to the strategy described in Subsection 3.2. In Subsection 3.3 investigations demonstrate the feasibility of the approach. Finally, in Section 4 conclusions are given.

2 TREES AS GENERALIZED ELLIPSOIDS OF REVOLUTION FITTED TO THE DSM

2.1 Model

Basically, the model consists of the semantic model for vegetation and the context. These two parts are on the semantic level and are more or less independent of the data employed for the extraction of the objects. Opposed to this, the geometric and radiometric representation is designed for trees which can be regarded as volumes, i.e., trees where the space between the branches and twigs is filled with needles or leaves.

2.1.1 Semantic Model for Vegetation

Although we have limited the actual extraction to trees and groups of trees, it is useful to relate them to other object types in the area of vegetation in the form of a semantic network [Brachman, 1977, Mayer, 1996]. The vegetation area (cf. Fig. 1) is specialized into plough-land, meadowland, group of trees, forest, shrubs, bushes, and other vegetation areas (e.g., moor-land). We restricted the detailed modeling to objects important for our goal. First, this is the group of trees. It consists of trees which can be specialized into either deciduous or coniferous trees. A special group of trees consists of trees planted in a row along a land use boundary or beside a road. The forest, which can be specialized into deciduous, mixed, and coniferous forest, consists above all of trees, but also of shrubs and bushes. Our modeling of shrubs and

bushes does not distinguish between them and represents them as one object "shrubs, bushes". A hedge is a special, i.e., linear form of this object.

An important way to come up with an as complete as possible modeling for an object, is to consider its function [Mayer, 1998]. For the object tree, e.g., its function in rows of trees is important. Rows of trees almost exclusively occur along land use boundaries or beside roads and serve as wind protection against soil removal or provide shadow against the heat. Additionally, rows of trees have an esthetic function in the form of avenues consisting of two rows of trees.

2.1.2 Context

We divide the context, which is according to [Mayer, 1998] made up from the interaction of the objects, into the local and the global context. In a so-called "local context", typical relationships between a few neighboring objects are formalized. The neighborhood is defined by local topology and geometry. For the tree, the following local contexts are important (the group and row of trees have been already mentioned in the semantic model for vegetation):

- Tree and shadow: The tree and its shadow are in a relationship to each other which can be clearly formalized: Every tree casts a shadow and the direction of the shadow results from the location of the tree and the time the aerial image was captured.
- Group of trees: Trees form groups if they stand close enough to each other.
- Row of trees: Trees form linear structures which possibly run parallel to other object types, such as roads.

The so-called "global context" consists of large areas and structure the local contexts as well as the objects. Opposed to [Mayer, 1998], the global context is viewed from different points of view. This leads to the following global contexts, which have an influence on the type of tree:

- Climatic zone: Depending on it, the common tree types vary considerably.
- Height above mean sea level (MSL): In the geographic latitude of Germany, coniferous trees are normally found only above a certain height above MSL. Isolated coniferous trees encountered in valleys have been planted by humans.
- Geomorphology and soil type: They influence the growth potential of different tree types. Not all tree types grow on a specific soil type.

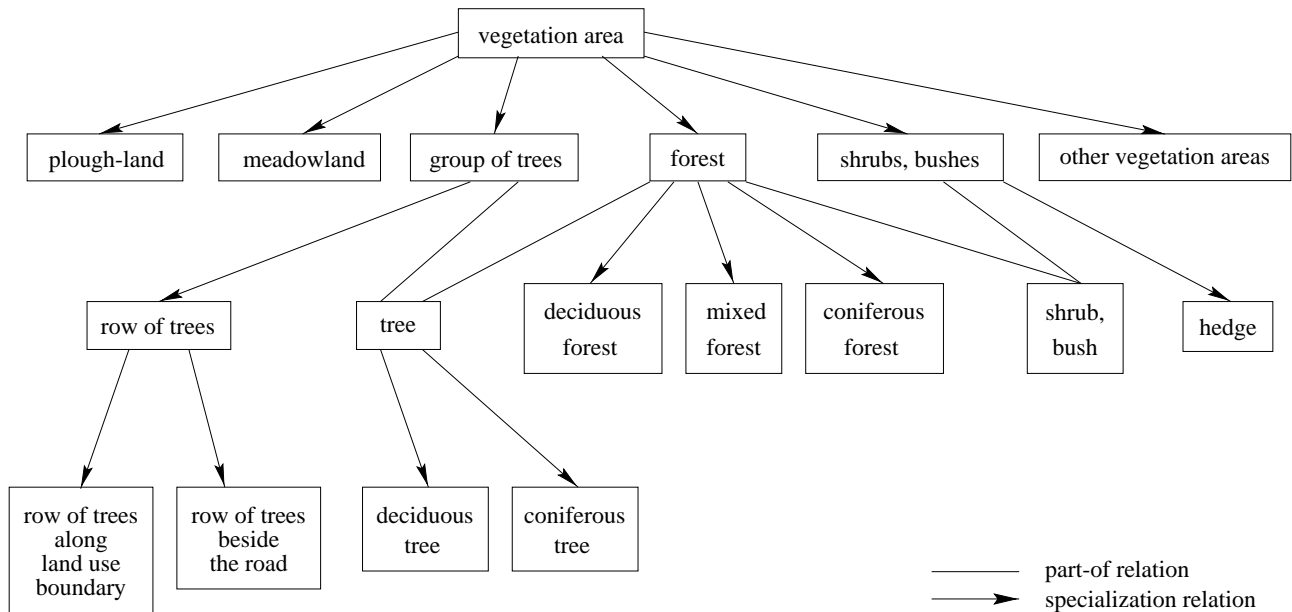


Figure 1: Model for vegetation

- Degree of cultivation: The degree of human intervention in the landscape and therefore also the occurrence of certain tree types is varying very much.
- Open rural area versus settlement (forest was already excluded above): Within settlements, foreign tree types might occur.

2.1.3 Coarse Geometrical Representation

Trees are modeled geometrically by generalized ellipsoids of revolution. This was already proposed and successfully employed for the representation of trees in aerial imagery in [Pollock, 1996, Larsen, 1998]. A generalized ellipsoid of revolution is defined mathematically as

$$\frac{z^n}{a^n} + \frac{(x^2 + y^2)^{\frac{n}{2}}}{b^n} = 1, \quad (28)$$

where a is the half length of the large axis and b of the small axis of the ellipsoid. With $r^2 = x^2 + y^2$, (28) can be transcribed to

$$\frac{z^n}{a^n} + \frac{r^n}{b^n} = 1. \quad (29)$$

(29) leads to:

$$\begin{aligned} \text{if } z = 0: & \quad r^n = b^n \quad \text{or} \quad |r| = b, \\ \text{if } r = 0: & \quad z^n = a^n \quad \text{or} \quad |z| = a \end{aligned} \quad (30)$$

with $a, b, n > 0$.

This means that the height of the tree corresponds to the half large axis a and the radius of the crown

to the small axis b of (28). In forest science, not the parameters a and b are employed for the identification of the tree type, but the ratio of tree height to the radius of the crown, i.e., a/b . This guarantees that a scaling factor depending on the age of the tree and influencing the amount of a and b is eliminated.

The parameter n is decisive for the shape of the generalized ellipsoid of revolution (cf. Fig. 2). From equation (29) it is clear that $n = 1$ results into the equation of a straight line $z = a - \frac{a}{b}r$. After rotation around the z axis, a cone is obtained. However, only the range $0 \leq z \leq a$ is of interest. For $n = 2$, the well-known formula of an ellipsoid of revolution is obtained from (28). For $n < 1$ and $n \rightarrow 0$, the object becomes increasingly concave and approaches the z axis as well as the xy plane. When we increase $n > 1$, the object becomes more and more convex and approaches a cylinder with radius b whose axis of rotation is the z axis and which is cut off at height $z = a$. Because different tree types, in particular deciduous and coniferous tree, can be distinguished by their shape, the parameter n is of great importance in forest science.

2.1.4 Radiometric Representation

The reflection of the light arriving at the tree directly from the sun and indirectly from the sky depends on:

- Tree type: The crown density function, which influences how much of the incoming light is reflected, is directly related to the tree type. On one hand, the reflection depends on the distance, the ray of light traveled in the tree before reflection. On the other hand, the leaves and branches as well as their composition have a great influence on the reflection.

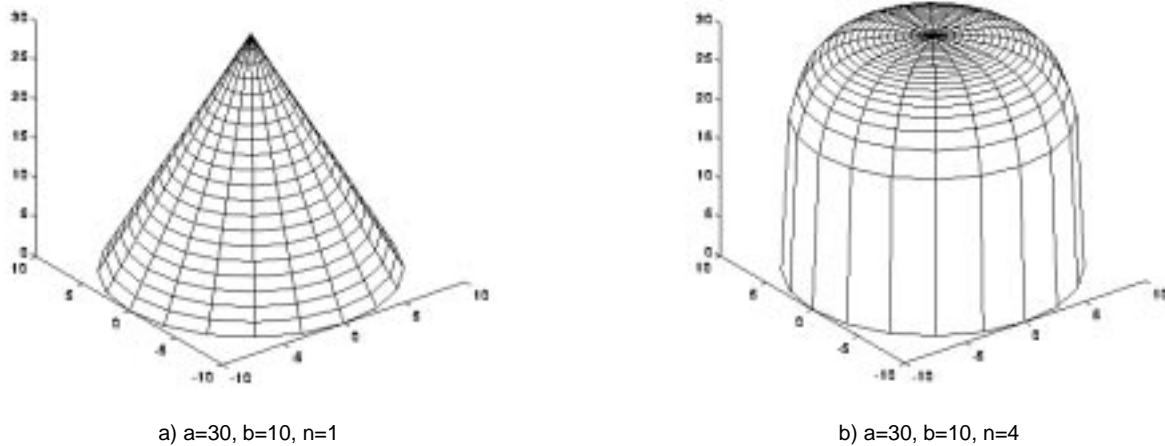


Figure 2: Generalized ellipsoid of revolution with different n

- Lighting conditions: The radiometric appearance of the tree depends on daytime, season, cloud density, etc.
- Resolution of the sensor: Every pixel of a tree projected into an image corresponds to a part of the real tree. Since the crown of a tree is not a closed face, it can happen, especially when using a high resolution, that the projected part represents only parts of the interior of the tree which are not lighted, and not the crown surface.

2.2 Strategy

We have split the extraction of trees in the two essential steps “detection of high textured objects” and “determination of the tree type”:

2.2.1 Detection of High Textured Objects

First, we extract areas corresponding to locally high objects from the DSM by means of criteria such as their width and their difference in height to neighboring areas. By including shape, texture, and color, natural and artificial, i.e., man-made, objects can be distinguished. Here, we did not implement this step because there are already at least partially successful approaches for it [Eckstein and Steger, 1996, Dissard et al., 1997] and we thought the following step to be more interesting.

2.2.2 Determination of the Tree Type

To unambiguously describe a tree with a generalized ellipsoid of revolution, the parameters a and b for the axes, the parameter n , and the center coordinates are enough. By means of optimally fitting a generalized ellipsoid of revolution into the area determined in the first step, it should be possible to derive the tree type from the ratio of the axes and the parameter n . Here, we assume that one area corresponds to exactly one object. Further sources of information are:

- texture/ (sub-)structure of the tree crown

- two-dimensional (2D) shape of the tree crown (outline)
- 2D shape of the shadow (outline)
- color

All these sources are typical for the tree type and are significantly different for different tree types. Due to the redundancy of the information sources, the derivation of the tree type should be possible. However, we estimate that the effort required for a formalization is very high.

2.3 Investigations

The central question is whether a DSM derived from automatic image matching is suitable for the classification of tree types for isolated trees? We approach this question by fitting a generalized ellipsoid of revolution to the DSM followed by a classification based on the shape parameter n .

On one hand, we chose the data in such a way that the determination of the tree type became possible. On the other hand, the data should reflect the situation encountered in practice. For the distinction of different tree types and, above all, for the determination of the degree of damage of a tree, color infrared images (CIR) are suitable [Albertz, 1991]. In forest science, CIR aerial images of scale 1:10 000 with normal angle objectives are employed. The Bavarian Landesanstalt für Wald- und Forstwirtschaft, Freising provided a stereo pair which we scanned with $15 \mu\text{m}$ resolution in all three channels. The images show an area south of Munich close to the Alps with mostly open and flat terrain (cf. Fig. 3).

We generated the DSM with PHODIS TS of Zeiss company, Oberkochen. A point density of 0.5 m was achieved. This corresponds to four to five pixels in the image at a ground pixel size of 12 cm. The smoothing



Figure 3: Part of the image “Bad Tölz” (permission granted from Bayerische Landesanstalt für Wald- und Forstwirtschaft, Freising)

of the DSM was carried out with the software package HIFI of Photogrammetrie GmbH, Munich [Ebner, 1992]. We examined two mesh widths: On one hand, 1.0 m, which has the advantage that mismatches do not influence the shape of the objects too much. However, trees situated close to each other may not be separable. On the other hand, we examined a DSM with 0.5 m mesh width. Here, in a first experiment, a high weight was given to the 3D points in the framework of the bilinear finite-element interpolation of HIFI (cf. Fig. 4). This preserved many of the mismatches. In a second experiment, we gave the smoothness condition, i.e., the second derivative is minimized, a high weight (cf. Fig. 5). This has the advantage that, on one hand, by means of the smaller mesh width the object is better represented than with a mesh width of 1 m and, on the other hand, on account of the higher weighting of the smoothness condition, disturbing information like mismatches are eliminated to a certain extent.

Into the DSM of the deciduous and coniferous tree we fitted generalized ellipsoids of revolution (cf. equation (28)) in an optimal way. I.e., we estimated the parameters a , b , and n as well as the center coordinates of the generalized ellipsoid of revolution by a least squares adjustment. For the given example (cf. Fig. 6) the ratio of a/b is 2.7 and 2.9, respectively. This means that the two ellipsoids of revolution are hardly distinguishable based on this ratio a/b alone. Things are different for the parameter n which reflects the shape of the ellipsoid of revolution. For the coniferous tree it is 1.8 and for the deciduous tree it is 2.5. I.e., it is clearly different. However, it should be noted as a limiting remark that this holds only for one data set. Further investigations with more data are necessary to verify the general hypothesis that at least decidu-

ous and coniferous trees are distinguishable from a DSM generated from an aerial image of scale 1:10 000.

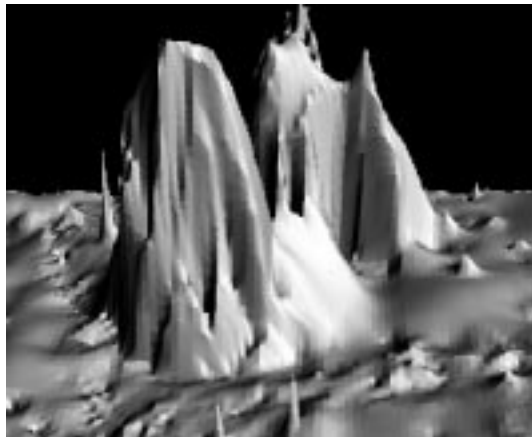
2.4 Assessment of the Approach

Up to this point we have shown that it might be possible to distinguish between deciduous and coniferous trees based on the coarse geometrical model, i.e., the generalized ellipsoid of revolution with its parameter n and the ratio a/b . However, for a more detailed classification of the tree type by means of the surface structure, the employed DSM appears not suitable. Above all, this is mostly due to the large amount of mismatches on account of the complex geometry and radiometry of the tree. Additionally, it is to be expected that this problem even increases when employing a finer resolution, since then more and more pixel look into the tree and not onto its surface, which makes matching more or less impossible.

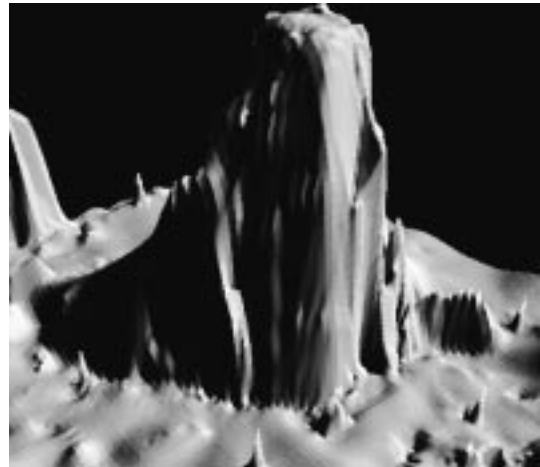
Additionally to the difficult interpolation of the DSM, further problems occur with the given data: The characteristic texture is a salient feature of deciduous trees (in leaf) and coniferous trees. [Shao and Förstner, 1994] demonstrates that there are great problems with the analysis of texture or (sub-) structure when interpreting images of natural scenes. In [Brandtberg, 1996] it is shown that the structure of the branches can be employed to classify the tree type. But this is feasible only for a much finer resolution, i.e., image scale of approximately 1:2000.

Another source of information for the determination of the tree type is the color of the crown in color or CIR aerial images. CIR images are employed for the determination of the degree of damage of a tree. Different tree types are often also distinguishable based on their color, however, mostly there are only small differences. This requires a data acquisition which preserves these differences. Even if the imaging is done completely digitally, the atmospheric conditions are known only to a certain degree, making a distinction of tree types by means of color information very difficult. By using multi- or even hyper-spectral data this disadvantage could be at least partially compensated by the big amount of information in the different wave bands.

Summing up, the determination of the tree type of isolated trees from automatically generated DSM is possible, but there are many factors which make it not too promising. Therefore, we took another direction to extract trees from aerial imagery as presented in the next Section.

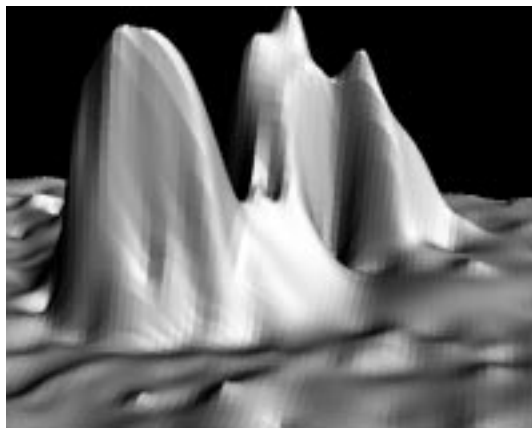


a) Coniferous tree

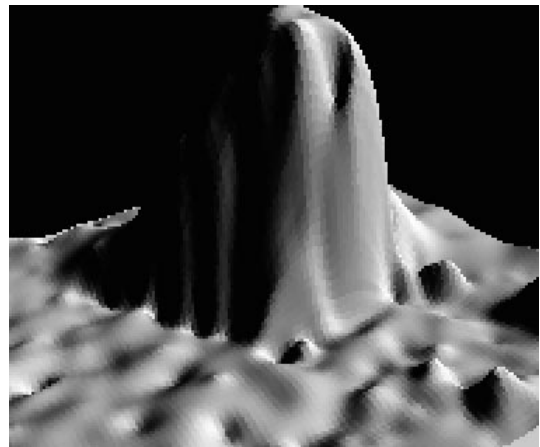


b) Deciduous tree

Figure 4: DSM – Mesh width 0.5 m and high weight of the matched points



a) Coniferous tree



b) Deciduous tree

Figure 5: DSM – Mesh width 0.5 m and high weight on the smoothness condition, i.e., the second derivative is minimized

3 DIRECT AND SHADOW PROJECTION OF LEAFLESS DECIDUOUS TREES

3.1 Model

We present our model of leafless deciduous trees in an aerial image with high resolution, i.e., 2-5 cm ground pixel size, as semantic network in Figure 7. The basic ideas for the modeling are similar to those used for building extraction, namely the utilization of dark shadows in sun direction¹, and the exploitation of vertical structures, i.e., especially the trunks, which are projected to nadir pointing straight lines [Jaynes et al., 1994, Lin and Nevatia, 1998, Shufelt, 1996]. Additionally, we assume that the deciduous tree is rotationally symmetric. Thus, its 3D outline can be derived from its normalized symmetric shadow projection.

In Figure 7 the deciduous tree is represented from

¹ i.e., projection of a vertical line on the horizontal ground, where the sun is the projection center

three different points of view, i.e., levels, which are connected by the so-called concrete link [Tönjes, 1997]: In the *real world*, the nearly rotationally symmetric tree consists of its trunk and crown. The base of the trunk is a part of the trunk and determines the position of the tree on the ground. The tree crown is connected to the trunk and consists of branches. The branches are connected hierarchically with decreasing thickness, ending in twigs.

In the *material and geometry* level the objects are described independently of the sensor. The trunk is represented as thick vertical, the branch as thin and mostly curved, and the twig as extremely thin wooden cylinder with a bark surface. The base of the trunk is a 3D point whose coordinates can be derived from two or more images or an existing digital terrain model (DTM).

On the *image* level, we represent the deciduous tree on one hand indirectly by its shadow projection and on the other hand by its direct projection. In shadow

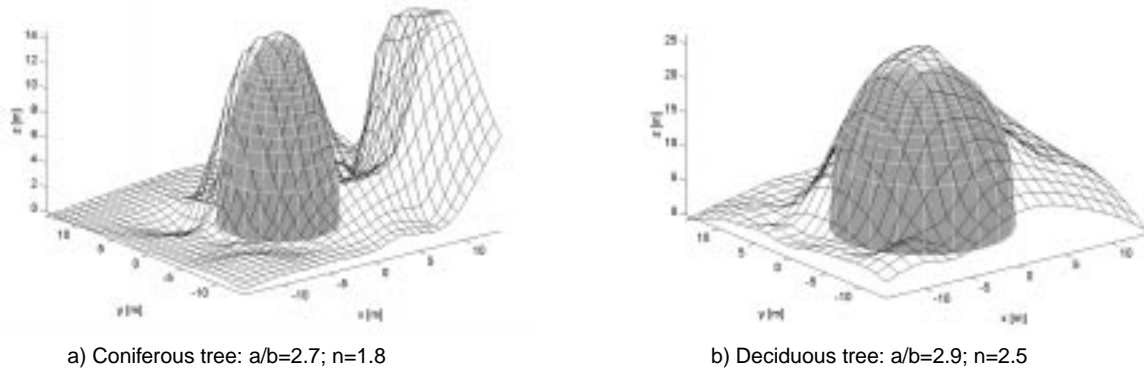


Figure 6: Estimated generalized ellipsoids of revolution

projection, the more or less vertical trunk appears as long distinct dark line in sun direction. The branches correspond to short dark lines of high contrast. The outermost thin twigs of the tree crown are not resolved at this resolution as lines, but appear as a blurred edge. In direct projection, the branches are short lines and the trunk is a long line in nadir direction. The lines are dark or light and mostly of low contrast.

By modeling also disturbing objects, we make the extraction robust. In the *real world*, they correspond to medium-sized volumes, e.g., cars, or they are vertical linear objects, such as poles and street-lamps. The latter can be modeled at the *material and geometry* level as vertical cylinders, which then appear in the shadow projection at the *image* level as long distinct dark lines. They are like the trunks directed in sun direction and can therefore be confused with them. The medium-sized volumes often appear as dark blobs disturbing the short dark lines of the branches and the blurred edge of the tree crown in shadow projection. To keep the model simple and compact, we decided not to integrate the occlusions by buildings and the shadows cast by them at this stage.

3.2 Strategy

Our strategy on top of the model is based on “hypothesize and verify”. We start with distinct dark lines in sun direction which are hypotheses for trunks. After the trunk is verified by integrating more and more evidence, we continue by tracking the branches, determination of the outline of the tree, and its classification.

3.2.1 Extraction and Verification of Hypotheses for Trunks

We start by extracting distinct dark lines representing the shadow projections of the trunks. Knowledge about existing objects, e.g., roads or buildings, may help to limit the search space geometrically, speeding up the extraction and making it more robust. Since the shadow of the trunk is oriented in sun direction, only

these lines are selected and combined to form hypotheses for trunks. The direct projection of the tree is employed as evidence to verify a hypothesis by extracting lines in nadir direction. Additionally, by intersecting the shadow of the trunk with its direct projection, the position of the base of a trunk can be determined more accurately and robustly. If the base is occluded, it might be recovered using only this second type of information.

3.2.2 Tracking of Branches and Determination of the Outline of the Tree

Using the information about the hypothesis for a shadow projection of a trunk, the dark lines representing the branches in shadow projection are extracted. This can be seen as a further verification of the hypothesis for the trunk.

From the end points of the branches together with the fact that the twigs form a blurred edge and the assumption that the shape of the tree is more or less compact and symmetric, the outline of the tree can be reconstructed using a snake-based approach. The diameter of the tree crown can be derived directly from the outline. The height can be computed from the known sun direction and the shadow outline projected onto the DTM.

3.2.3 Derivation of the Tree Type

The tree type is derived by a classification based on the shape of the outline, the ratio of the width of the tree crown and the height of the tree, and the structure of the branches.

3.2.4 Limitations of the Strategy

We have outlined the proposed strategy for one gray-scale image only. We do not use color information, because the shadow has no color and the trunk is only weakly colored. In principle, $n \geq 2$ images might be used to find corresponding structures of the branches. We have not done this due to the following reasons: Matching the shadow projection only results in a refined DTM. By matching the direct projection of the branches in two or more images, the

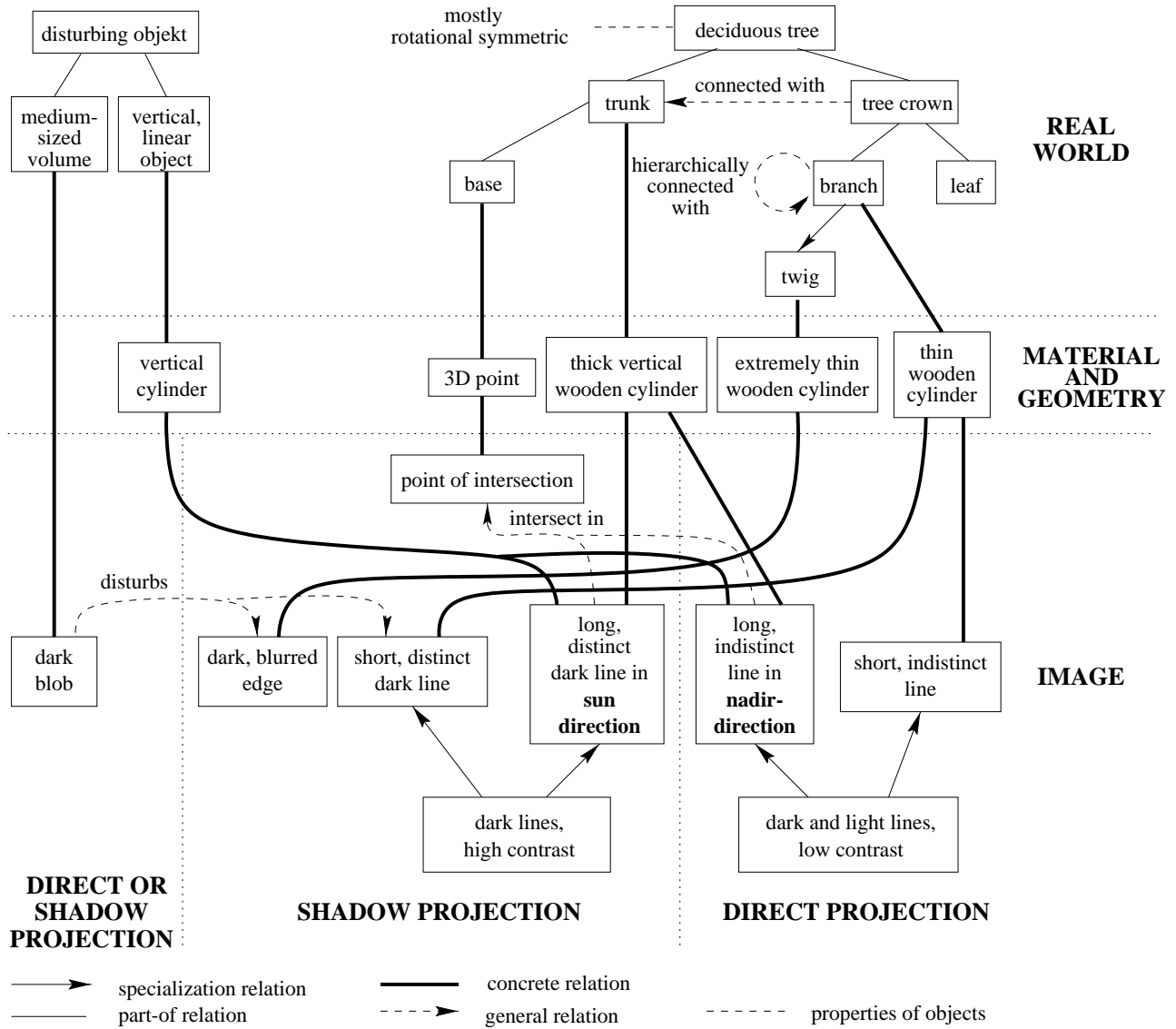


Figure 7: Model for leafless deciduous tree and disturbing object

3D branching structure could be reconstructed. However, there are not only tight limits in line extraction, but above all, the complexity of matching these structures is extremely high. Contrary to this, the information for our application can be derived which much less effort from the shadow projection of the tree.

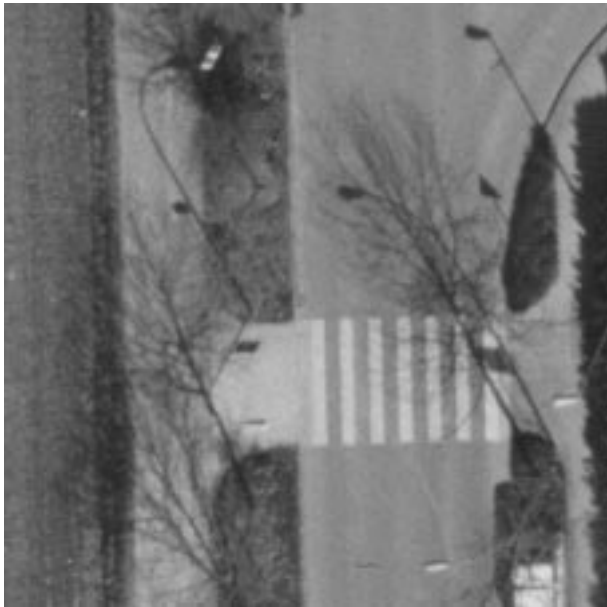
3.3 Investigations

Figure 8 shows a part of an image representing a suburban area of the German town Tamm near Stuttgart. The image was scanned at a pixel size of 14 μm corresponding to a pixel size of 4.2 cm on the ground at an image scale of 1:3000. The image was taken in early spring. The shadows of the trees are mostly cast on roads and clearly show the structure of the branches.

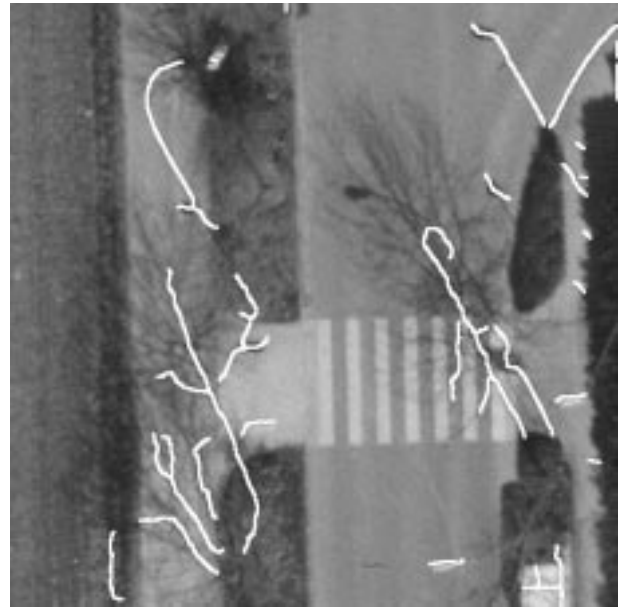
3.3.1 Hypotheses for Trunks

First, we extract distinct dark lines (cf. Fig. 9b) with a line extractor based on differential-geometry and the Gaussian scale-space [Steger, 1998]. To determine the hypotheses for trunks, we make use of the following properties of their shadow projection: a) Trunks are represented by relatively long straight lines. b) The lines representing trunks are oriented in sun direction. As position and attitude of the image as well as the date and time of its acquisition are known, the sun direction could be computed. We have estimated it directly from the image.

A typical application of the Hough transform [Ballard and Brown, 1982] is the detection of straight lines in a specific direction. We apply it with the two parameters distance from the origin and orientation. Hypotheses for trunks are local maxima of an interval around the sun direction. In Figure 10a) the local maxima have been projected back into the image as straight lines.



a) Part of the image



b) Distinct dark lines

Figure 9: Extraction of dark lines with high contrast

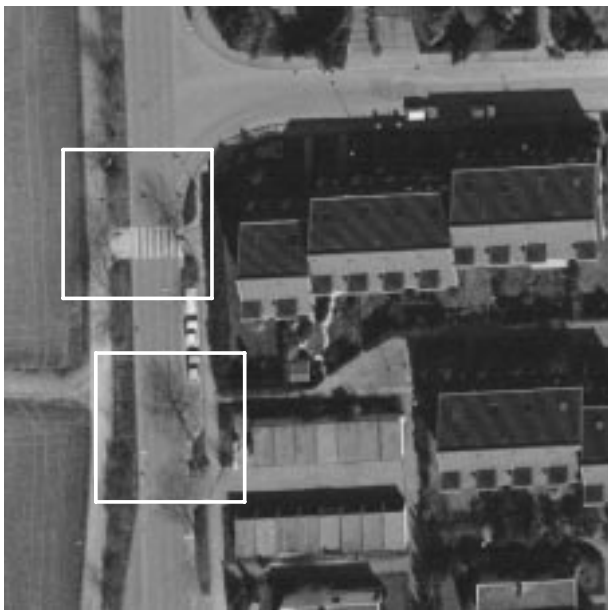


Figure 8: Part of the image Tamm (image courtesy of Photogrammetrie GmbH, Munich)

The dark lines are oriented in sun direction and are called “Hough-lines” for the remainder of the paper.

In a next step, the lines in the image which are represented by the Hough-lines are selected and connected by morphological closing [Serra, 1982]. Short lines are eliminated because they cannot correspond to trunks. For the remaining lines straight lines are computed by regression. Unfortunately, they can also correspond to the shadow projections of disturbing objects (cf. Fig. 10b). The results demonstrate that the extraction of the trunk is feasible, though it still has to

be refined. For example, hypotheses for trunks can be tracked in sun direction to find lines with low contrast.

3.3.2 Direct Projection of the Trunk in Nadir Direction

Contrary to shadows, which are always darker than the surroundings, the direct projection of the trunk can be both, lighter as well as darker. Therefore, we extract dark as well as light lines. Then, we use the same procedure based on the Hough transformation as described above for the selection of lines in nadir direction. Ideally, finally one single long line represents the direct projection of the trunk. Figure 11a) shows in black the search areas for the hypotheses for trunks presented in white. One direction of the parallelogram is determined by the shadow projection, the other by the direction to the nadir point. The lengths are the same as for the hypotheses for the trunks. The extracted lines within the search areas and the extracted lines pointing in nadir direction are illustrated in grey and white, respectively. The procedure is successful for the street-lamp on the top-left and for the trunk on the bottom-right. However, a refinement is still necessary.

3.3.3 Branches in Shadow Projection

The extraction of branches in the shadow projection is geometrically restricted using the hypotheses for the trunks. It makes use of the properties of the chosen line extraction. The search areas are defined by ellipses with the hypotheses for the trunks defining their longer axes. The smaller axes have half the length. Within these ellipses distinct dark lines are extracted (cf. Fig. 11b). We exploit the knowledge that branches are starting at the trunk and are of

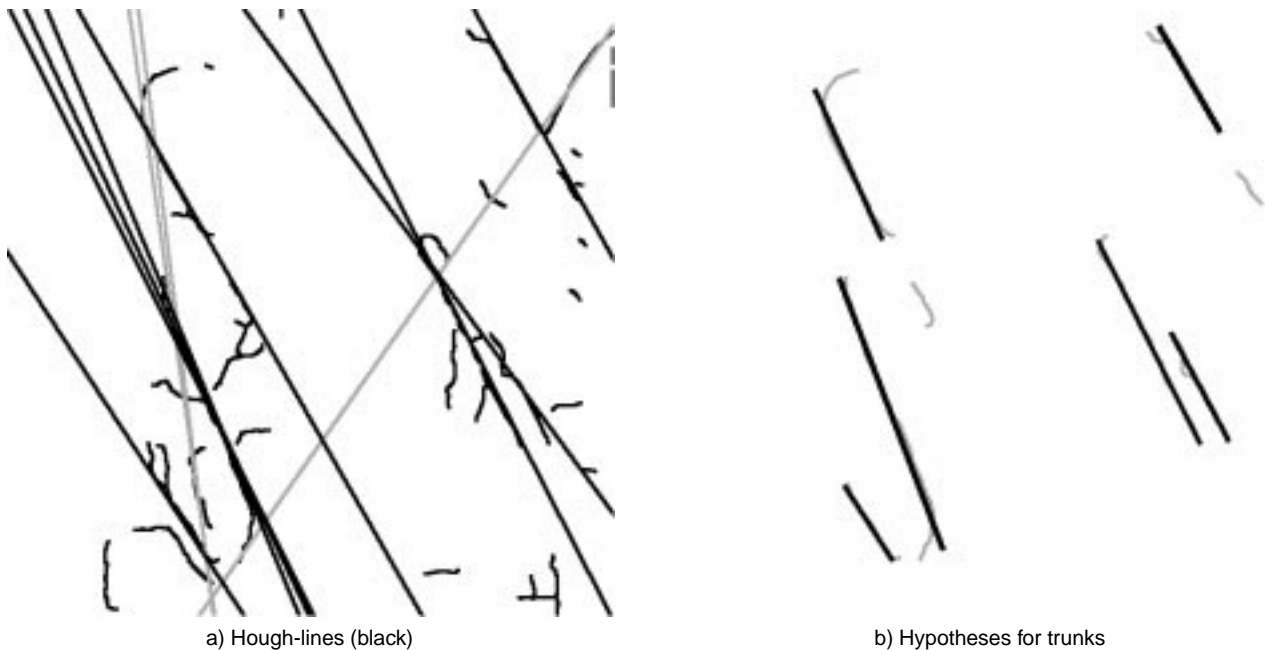


Figure 10: Result of Hough transformation and Hypotheses for trunks

decreasing thickness by exploiting hysteresis thresholding [Canny, 1986] in the following way: The upper threshold is set very high to obtain only lines with high contrast, i.e., the trunk, as starting points. On the other hand, the lower threshold is chosen relatively low, to track branches to their final ends. Only light smoothing is used in the image to detect also very thin lines. As the used version of the line extractor does not work recursively, at every branching only one line is tracked. Figure 12 shows the results for two different hypotheses for trunks for another part of the image. In one case, the hypothesis represents the trunk of a deciduous tree, but in the other case a disturbing object, i.e., a street-lamp.

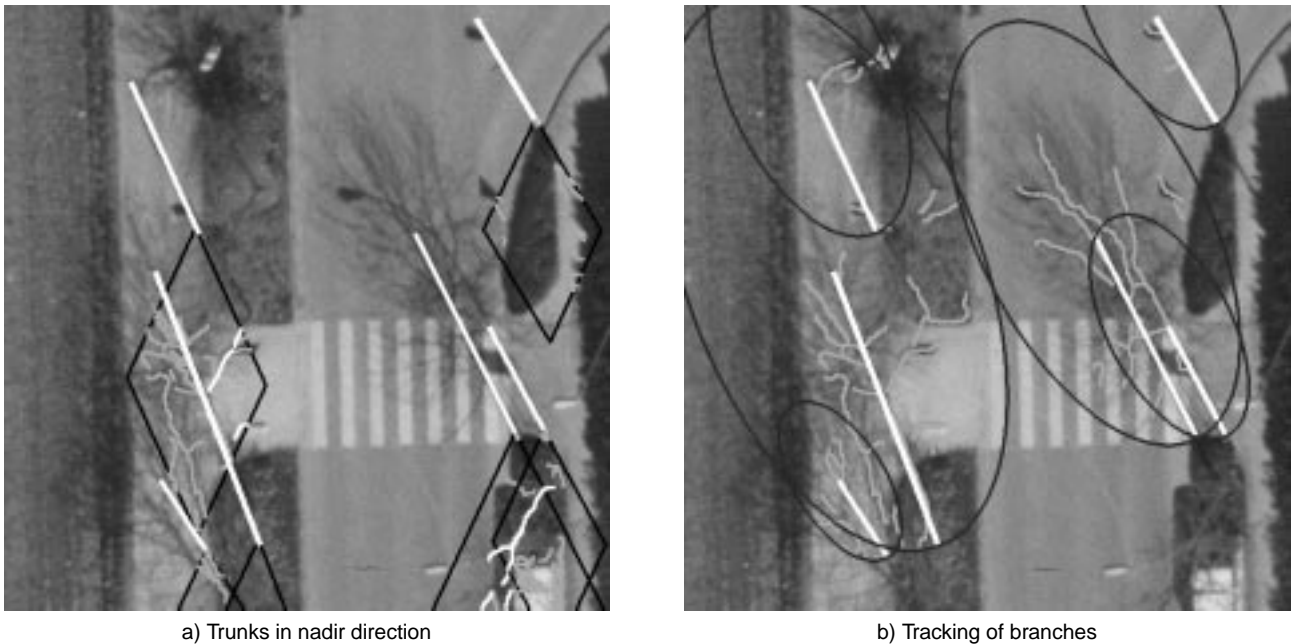
4 CONCLUSIONS

We have presented two approaches for the automatic extraction of trees from aerial imagery. Both have different areas of application: While the first one works for any tree type, it is restricted to isolated trees and therefore applicable only to (open) rural areas. We have demonstrated that the extraction from the DSM based on the generalized ellipsoid of revolution is feasible, but has tight limits in terms of potential for automation. Therefore, we decided to have a look on other ways to extract trees. We have found that it is often feasible to extract leafless deciduous trees from high resolution aerial imagery of suburban areas from their shadow and their direct projection. Even branches can be extracted at a ground pixel size of about 4 cm. For this approach we plan to expand the tracking of the branches to all possible lines. Already at this stage trees and disturbing objects will be distinguished based on the extracted branches. Addi-

tionally, we want to determine the outline based on the end points of the branches, the blurred edge defined by the shadow projection of the twigs, and the compactness of the tree crown using snakes. Summing up, we expect that the parameters nowadays collected manually, like the height of the tree, the width of the tree crown, the base of the trunk, and after a classification also the tree type, can then be determined fully automatically.

REFERENCES

- [Albertz, 1991] Albertz, J., 1991. Grundlagen der Interpretation von Luft- Satellitenbildern. Wissenschaftliche Buchgesellschaft Darmstadt.
- [Ballard and Brown, 1982] Ballard, D. and Brown, C., 1982. Computer Vision. Prentice-Hall International, Englewood Cliffs, USA.
- [Baumgartner, 1998] Baumgartner, A., 1998. Extraction of Roads from Aerial Imagery Based on Grouping and Local Context. In: International Archives of Photogrammetry and Remote Sensing, Vol. (32) 3/1, pp. 196–201.
- [Brachman, 1977] Brachman, R., 1977. What's in a Concept: Structural Foundations for Semantic Networks. International Journal of Man-Machine Studies 9, pp. 127–152.
- [Brandtberg, 1996] Brandtberg, T., 1996. Automated Tree Species Classification in High Resolution Aerial Images Using a Hough Transform Technique. In: Swedish Symposium on Image Analysis.



a) Trunks in nadir direction

b) Tracking of branches

Figure 11: Direct projection of trunks in nadir direction and tracking of branches (a): Hypotheses for trunks from shadow projection = white; search area = black parallelogram; lines = grey; lines in nadir direction = white b): Search area = black ellipse; branches = grey lines)

[Canny, 1986] Canny, J., 1986. A Computational Approach to Edge Detection. *IEEE Transactions on Pattern Analysis and Machine Intelligence* 8(6), pp. 679–698.

[Dissard et al., 1997] Dissard, O., Baillard, C., Maître, H. and Jamet, O., 1997. Above Ground Objects in Urban Scenes from Medium Scale Aerial Imagery. In: *Automatic Extraction of Man-Made Objects from Aerial and Space Images (II)*, Birkhäuser Verlag, Basel, Schweiz, pp. 183–192.

[Ebner, 1992] Ebner, H., 1992. Digital Terrain Models and their Applications. *GIS* 5(3), pp. 27–30.

[Eckstein and Steger, 1996] Eckstein, W. and Steger, C., 1996. Fusion of Digital Terrain Models and Texture for Object Extraction. In: *Second International Airborne Remote Sensing Conference and Exhibition*, Vol. III, pp. 1–10.

[Jaynes et al., 1994] Jaynes, C., Stolle, F. and Collins, R., 1994. Task Driven Perceptual Organization for Extraction of Rooftop Polygons. In: *2nd IEEE Workshop on Applications of Computer Vision*, pp. 152–159.

[Larsen, 1998] Larsen, M., 1998. Finding an Optimal Match Window for Spruce Top Detection Based on an Optical Tree Model. In: *International Forum on Automated Interpretation of High Spatial Resolution Digital Imagery for Forestry*, 10.-12.02.1998, Victoria, B.C., Kanada.

[Lin and Nevatia, 1998] Lin, C. and Nevatia, R., 1998. Building Detection and Description from a Single In-

tensity Image. *Computer Vision and Image Understanding* 72(2), pp. 101–121.

[Mayer, 1996] Mayer, H., 1996. Using Real World Knowledge for the Automatic Acquisition of GIS-Objects from Scanned Maps. *GIS* 9(2), pp. 14–20.

[Mayer, 1998] Mayer, H., 1998. Automatische Objektextraktion aus digitalen Luftbildern. *Deutsche Geodätische Kommission (C) 494*, München.

[Pollock, 1996] Pollock, R., 1996. The Automatic Recognition of Individual Trees in Aerial Images of Forests Based on a Synthetic Tree Crown Image Model. PhD Thesis, The Faculty of Computer Science, The University of British Columbia, Vancouver, Kanada.

[Serra, 1982] Serra, J., 1982. *Image Analysis and Mathematical Morphology*. Academic Press, London, Großbritannien.

[Shao and Förstner, 1994] Shao, J. and Förstner, W., 1994. Gabor Wavelets for Texture Edge Extraction. In: *International Archives of Photogrammetry and Remote Sensing*, Vol. (30) 3/2, pp. 745–752.

[Shufelt, 1996] Shufelt, J., 1996. Exploiting Photogrammetric Methods for Building Extraction in Aerial Images. In: *International Archives of Photogrammetry and Remote Sensing*, Vol. (31) B6/VI, pp. 74–79.

[Steger, 1998] Steger, C., 1998. An Unbiased Extractor of Curvilinear Structures. *IEEE Transactions on Pattern Analysis and Machine Intelligence* 20, pp. 113–125.



a) Hypothesis for trunk no. 1



b) Hypothesis for trunk no. 2

Figure 12: Branches for different hypotheses for trunks

[Tönjes, 1997] Tönjes, R., 1997. 3D Reconstruction of Objects from Aerial Images Using a GIS. In: International Archives of Photogrammetry and Remote Sensing, Vol. (32) 3-2W3, pp. 140–147.